Toxicology Research

Accepted Manuscript

ROYAL SOCIETY OF CHEMISTRY

www.rsc.org/toxicology

Toxicology Research

Paper

Biocompatibility of graphene oxide post intravenously administrated in mice－－effects of dose, size and exposure protocol

Jia-Hui Liu,[a,b,c] Tiancheng Wang,[d] Haifang Wang,*[b] Yongen Gu,[e] Yingying Xu,[a] Huan Tang,[a] Guang Jia[e] and Yuanfang Liu*[a,b]

Graphene oxide (GO) shows great promise in the *in vivo* drug delivery and therapy applications. In the meantime, several reports have reported the *in vivo* toxicity of GO. In this study, we found that the toxicity of GO intravenously injected into mice could be tuned by the dose, size and exposure protocols [10] of GO. The exposure with a single dosing of 2.1 mg kg^{-1} (single-high-dose exposure) of small size GO or large size GO caused the macrophage nodules formation in lungs in mice, and the exposure with seven repeated dosing of 0.3 mg kg^{-1} (multiple-low-dose exposure) of large size GO also induced small macrophage nodules formation, serious lymphocyte infiltration around the bronchioles in lungs in mice, and even the death of mice. The nephritic inflammatory reactions were also observed after multiple-low-[15] dose exposure of large size GO. However, no obvious lung toxicity but hepatic inflammatory infiltration was observed in the exposure with multiple-low-dose of small size GO. GO accumulation in macrophage nodules was verified by Raman mapping. These findings will benefit the applications of GO in future, especially in the biomedical fields.

Introduction

[20] The rapid development in nanotechnology has spawned numerous novel applications and products. The subsequent issues on the biosafety of the new nanomaterials are attracting more and more attentions.[1,2] A number of researches have been conducted on the biological effects of nanomaterials, such as carbon [25] nanomaterals, polymer nanoparticles and quantum dots, at both *in vitro* and *in vivo* levels.[3-5] After over a decade exploration, the researchers realized that the biological effect of nanomaterials is complex, and is largely affected by the exposed dose, exposure methods as well as the nature of the materials, e.g. chemical [30] composition, size, structure and surface properties.[5-7]

Very recently, the newly developed material graphene and its derivatives have become one research focus due to their unique properties in electronics, chemistry, mechanics, and two-dimensional carbon structure.[8,9] Among the graphene derivatives, [35] graphene oxide (GO) has been widely explored for *in vitro* and *in vivo* drug delivery and imaging, taking advantage of its high solubility and stability in physiological solutions, low cost and scalable production, and facile biological/chemical functionalization.[10-14]

[40] However, the biocompatibility of GO is inconclusive. Several studies supported its good biocompatibility.[15-18] Nevertheless, granuloma formation, inflammation, and thrombus formation in mice have also been observed after GO exposure.[19-22] The different experiment conditions and GO characters, such as [45] exposure methods, dose, GO size and surface properties, may be

reasons for the inconsistence. Small size GO, especially after modification, was reported to be more biocompatible at the low concentration.[15-18,23] Nevertheless, the large delocalized-election system, which is always essential for their biological [50] applications,[24] might be damaged by chemical modification. A high dose exposure of GO would be needed for its application, that could therefore induce toxicity. Multiple-low-dose injection is always an alternative method for drugs that are not appropriate for the single-high-dose injection. Actually, many nanotoxicity [55] researches have been done by the multiple-injection but inconsistent results were obtained.[25-28] Therefore, a systematic safety evaluation of nanomaterials using multiple-injection as well as the comparison between the single and multiple injection are essential for the bioapplications of GO.

[60] Herein, we report the effects of size, dose and dosing frequency on the toxicity of GO in mice. Mice were exposed intravenously (*i.v.*) to GO and saline control following Scheme 1, which diagrams the exposure schedule, i.e. mice were given the single-dose of 0.3 mg kg^{-1} or 2.1 mg kg^{-1}, or the multiple-dose of [65] 0.3 mg kg^{-1} every other day for 15 days. After *i.v.* exposure, the toxicity of GO in main organs, including liver, lungs, kidneys and spleen, were evaluated to provide a general toxicological profile of GO in mice. It was found that the multiple-low-dose exposure of small size GO was safer to mice.

2. Materials and methods

2.1 Preparation and characterization of GOs

Both s-GO (small size GO) and l-GO (large size GO) were

prepared and characterized carefully following our previous report.[6] Briefly, GO suspension, prepared following the modified Hummers method (see Supplementary Information (SI)), was further heated at 120 °C for 20 min to generate small GO sheets. The obtained suspension was centrifuged at 36,000 g for 50 min to separate s-GO (supernatant) and l-GO (residue). GO samples were dispersed in ultrapure water to prepare the stock suspension (1.0 mg mL^{-1}). The concentration of GO samples was measured by drying and weighing GO in an aliquot of suspension.

The shape and thickness of GO sheets were characterized by atomic force microscopy (AFM; SPM-9600, Shimadzu, Japan). The particle size distribution and ζ-potential of GO in water were measured by a nanosizer (DLS, NanoZS90, Malvern, UK).

Single-dose

Multiple-dose

Examination
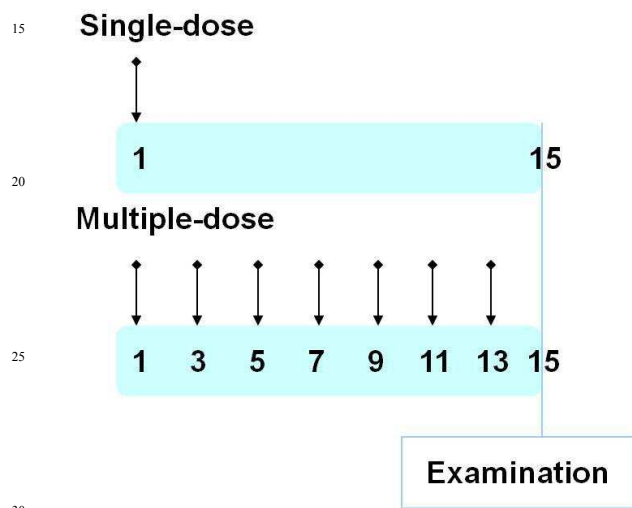
Scheme. 1 Animal exposure schedule. ICR mice were *i.v.* injected with GO or 0.9% saline. For single-dose exposure, mice were given either 0.3 mg kg^{-1} or 2.1 mg kg^{-1} s-GO or l-GO; for multiple-dose exposure, mice were given seven times of 0.3 mg kg^{-1} s-GO or l-GO every other day. Examinations were performed on day 15.

2.2 Animal exposure and sampling

All animal experiments were performed in compliance with the institutional ethics committee regulations and guidelines on animal welfare (Animal Care and Use Program Guidelines of Peking University), and approved by Peking University.

Male CD-1 (ICR) mice (~25 g) were obtained from Peking University Animal Center, Beijing, China. They were housed in plastic cages (five mice per cage) and kept on a 12 h light/dark cycle. Food and water were provided *ad libitum*. After acclimation, mice were randomized into groups.

Mice were *i.v.* injected with GO suspensions and the saline control through the tail vein following Scheme 1. The body weight and behaviours were recorded every day post first exposure.

At day 15, mice were sacrificed and blood/organ samples were collected for toxicological assays. Blood plasma samples were collected from blood (1.0 mL) by anti-coagulation with sodium citrate (0.1 μL 3.2% (w/v)) and centrifugation (3000 g for 10 min). Liver, lungs, spleen and kidneys were collected and weighed for organ indices (organ weight/body weight) calculation. Two pieces of each organ were cut off and fixed in 4% formaldehyde solution. The rest were stored at -80 °C.

2.3 Determination of plasma coagulation and biochemical parameters

Following the standard procedures activated partial thromboplastin time (APTT) and fibrinogen (Fib) were measured with an automated coagulometer (ACL 9000, Instrumentation Laboratory, Lexington, USA). Biochemical assays were performed using a Hitachi 7170A clinical automatic chemistry analyzer (Hitachi Ltd., Tokyo, Japan). Lactate total bilirubin (TBIL), alanine aminotransferase (ALT), aspartate aminotraferase (AST), alkaline phosphates (ALP), uric acid (UA), urea (UREA), creatinine (CRE) and dehydrogenase (LDH) were measured using the commercial kits (Bühlmann Laboratories, Switzerland).

2.4 Histological observations

For histological observations, the formalin-fixed tissue samples were embedded in paraffin, thin-sectioned and mounted on glass microscope slides for hematoxylin-eosin (H&E) staining and followed examination by light microscopy.

2.5 Apoptosis assay

Cell apoptosis of organs was evaluated by using the terminal deoxynucleotidyl transferasemediated dUTP nick-end-labeling (TUNEL) technique on the organ sections. All the reagents used were purchased from Dingguo Biotechnology Co., Beijing, China and the instruction was followed exactly as described in our previous work.[29]

2.6 Oxidative stress assay

For the assays of the reduced glutathione (GSH) level and malondialdehyde (MDA) level, each organ sample was minced and homogenized in 4 °C for three times (10 s each time, intermittent for 30 s) to yield a 10% (w/v) homogenate. The homogenates were centrifuged at 3000 g for 10 min to obtain the supernatants. The protein concentration of the supernatants was determined with the method of Bradford, using the bovine serum albumin as the standard. The reduced GSH level of the supernatants was examined by using spectrophotometric diagnostic kits (Nanjing Jiancheng Biotechnology Institute, China). Results of GSH are expressed as mg GSH (g protein)$^{-1}$. The lipid peroxidation indicator MDA was determined by the method of thiobarbituric acid reactive species (Nanjing Jiancheng Biotechnology Institute, China). The levels of MDA are expressed as nmol MDA (mg protein)$^{-1}$ using 1,1,3,3-tetraethoxypropane (TEP) as the standard. The measurements of GSH and MDA were performed following the manufacturer's instructions.

2.7 Micro-Raman mapping of GOs in lung tissues

The lung tissue slides were focused in Raman microscope (Renishaw, UK) at × 20 magnification and excited with 785 nm laser (100 mW). Images were obtained by scanning an area in 7 μm × 7 μm steps, collecting the Raman spectrum at each spot (2 s integration time), and plotting the integral of the area under G-peak (around 1600 cm^{-1}, characteristic peak of GO) in the corresponding spot to form the area image. Both the H&E staining slide and apoptosis assay slide of lung tissues were measured.

2.8 Statistical analysis

All data are presented as the mean of more than three individual observations with the standard deviation. Significance has been calculated using the Student's t-test. Difference is considered significant if p < 0.05.

3. Results

3.1 GO samples

Both s-GO and l-GO used in this work are the same as those in our previous paper.[6] The GO sheets showed typical G-band (1600 cm^{-1}) in the Raman spectrum and similar contents of oxygen-containing groups. Most GO sheets were single layers (the thickness is around 0.9 nm), and had a size in the range of several micrometer for l-GO (2.2 ± 1.4 μm) and 0.54 ± 0.26 μm for s-GO (Fig. S1 in SI). In water suspension, the average hydrodynamic diameter were 914 nm for l-GO and 243 nm for s-GO. In a word, the two GO samples have very similar properties except for the size.

3.2 Effects of GO on mouse death, body weight and organ indices

We found that the mice can hardly live 2 weeks after one single intravenous injection of 10 mg kg^{-1} b.w. GO. Zhang *et al.*
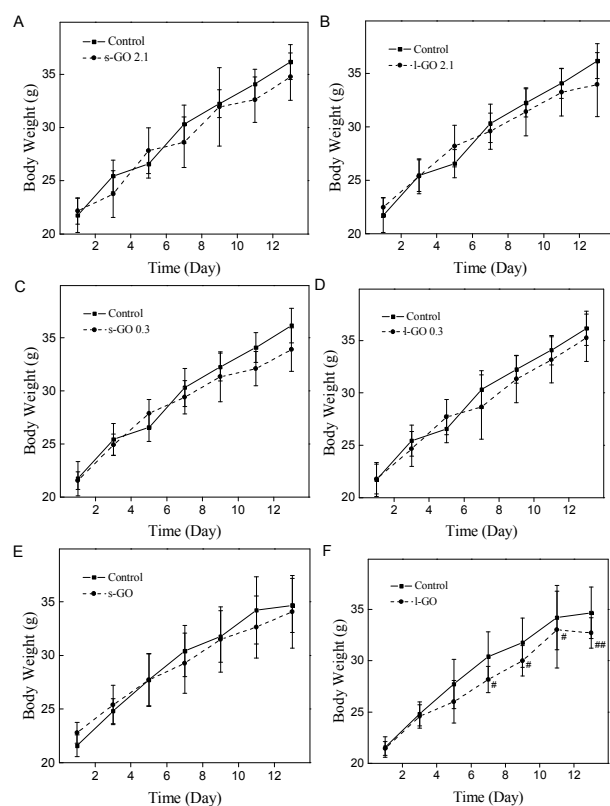

also reported that mice treated with 10 mg kg^{-1} b.w. GO for 14 day induced significant pathological changes, including granulomatous lesions, pulmonary edema, inflammatory cell infiltration and fibrosis throughout the lungs, due to the high accumulation and low clearance of GO in mice.[22] In addition, we found that the biodistribution of GO could be dramatically tuned by the concentration of GO and 2 mg kg^{-1} b.w. is a transitional dose, where the biodistribution is significantly different from 1 mg/kg b.w. GO.[6] Therefore, 2.1 mg kg^{-1} b.w. (the single dose of 2.1 mg kg^{-1} b.w. and the seven-repeated dose of 0.3 mg/kg b.w.) was chosen as the high dose in this study.

In the multiple-dose l-GO group, two mice were found dead on day 8 and one more dead on day 13. The mice in this group exhibited the following clinical abnormality: Thin appearance, fur-upright and less movement. No abnormal clinical signs or death was found in other groups and all these mice were in good condition at the time of sacrifice.

The effects of GO on body weight and organ indices of liver, lungs spleen and kidneys were monitored. The body weights of GO treated mice don't show any significant difference from those of the control mice (Fig. 1). Although, the body weights of multiple-dose l-GO group mice were slightly (but not significant) lower than those of the control and multiple-dose s-GO group mice.

The organ indices are commonly used in the toxicological evaluation to provide a general impression of toxicity. The data are summarized in Table 1. No organ index of the single-dose groups is significantly changed comparing with the control group. Neither size nor dose alters the organ indices after the single-exposure. However, the size-related change of the organ index is observed in mice post the multiple-dose exposure of GO. The liver index of the multiple-exposure of s-GO is significantly lower than that of the control group, which means the organ atrophy or degenerative changes, etc., but its lung index is not markedly changed. Conversely, for the multiple-dose exposure of l-GO, the lung index is significantly higher than that of the control, which means the organ congestion, edema or hypetrophy, etc., but the liver index keeps unchanged. It has been reported that the distribution of GO in liver and lungs was size-dependent, s-GO mainly accumulated in liver, and l-GO mainly accumulated in lungs.[6] Clearly, the GO size-related change in liver and lung indices closely relates with the GO accumulation in these organs. No obvious difference is observed in spleen and kidney indices among all groups.

3.3 Effects of GO on plasma coagulation and biochemical parameters of mice

It has been reported that GO induced thrombi after *i.v.* exposure.[20,21] Therefore, the plasma coagulation parameters were assayed to evaluate the toxicity of GOs in blood. Table 2 shows the typical coagulation parameters Fib (fibrinogen) and APTT (activated partial thromboplatin time). However, the levels of Fib and APTT keep normal, regardless of GO samples and dosing frequency. The finding is in accordance with Sasidharan *et al.*'s conclusion that graphene was nonthrombogenic by testing the possibility of graphene interference with the prothrombin time (PT) and activated partial thromboplastin time ratio (APTTr).[17]

Fig. 1 Body weights of mice *i.v.* injected with s-GO, l-GO or saline in 15 days from the first injection (n=8, except specified). (A) Sing-dose of s-GO at 2.1 mg kg^{-1} (s-GO 2.1) was compared with the single dose control; (B) Sing-dose of l-GO at 2.1 mg kg^{-1} (l-GO 2.1) was compared with the single dose control; (C) Sing-dose of s-GO at 0.3 mg kg^{-1} (s-GO 0.3) was compared with the single dose control; (D) Sing-dose of l-GO at 0.3 mg kg^{-1} (l-GO 0.3) was compared with the single dose control; (E) Multiple-dose of s-GO at 0.3 mg kg^{-1} (s-GO) was compared with the multiple-dose control; (F) Multiple-dose of l-GO at 0.3 mg kg^{-1} (l-GO) was compared with the multiple-dose control.($^{\#}$ n=6, $^{\#\#}$ n=5).

Table 1. Organ indices of the GO-exposed and control mice. Data represent mean±S.D. (n=5).

Animal groups		Organ indices[a] (mg g^{-1})			
		liver	lungs	spleen	kidneys
Single-dose	Control	57±2	5.2±0.6	4.3±1.0	16±1.0
	0.3 mg kg^{-1} s-GO	54± 3	6.5± 0.6	5.0±1.1	16±1.0
	0.3 mg kg^{-1} l-GO	52± 6	6.6± 0.4	4.5± 0.4	16± 2.0
	2.1 mg kg^{-1} s-GO	50 ± 4	6.5± 0.6	4.9±0.6	16± 0.9
	2.1 mg kg^{-1} l-GO	58± 4	6.9±1.1	4.8± 0.7	16±0.5
Multiple-dose	Control	59± 2	6.9± 0.5	5.6±0.7	16± 0.8
	0.3 mg kg^{-1} s-GO	54 ±3*	6.8± 0.7	6.1±0.9	15± 1.0
	0.3 mg kg^{-1} l-GO	60 ± 5	8.0±0.3*	7.2±2.0	15±1.0

[a](organ weight/body weight)×1000.
* Significant different from the control at P<0.05.

5

Table 2. Plasma coagulation parameters of the GO-exposed and control mice. Data represent mean±S.D. (n=5).

Animal groups		Fib (g L^{-1})	APTT(s)
Single-dose	Control	3.09± 0.30	21.8± 2.1
	0.3 mg kg^{-1} s-GO	2.82± 0.43	24.8± 3.5
	0.3 mg kg^{-1} l-GO	3.12± 0.74	23.3± 2.6
	2.1 mg kg^{-1} s-GO	2.89± 0.18	22.0± 2.1
	2.1 mg kg^{-1} l-GO	3.10 ± 0.32	21.3± 0.8
Multiple-dose	Control	3.26± 0.30	23.7± 1.5
	0.3 mg kg^{-1} s-GO	2.88± 0.19	20.7± 1.9
	0.3 mg kg^{-1} l-GO	2.94± 0.22	21.7±2.5

Fib: fibrinogen; APTT: activated partial thromboplatin time.

Next, the plasma biochemical parameters were measured and the results are summarized in Table 3. After GO injection, the levels of biochemical parameters, including lactate total bilirubin (TBIL), alanine aminotransferase (ALT), aspartate aminotraferase (AST), alkaline phosphates (ALP), uric acid (UA), urea (UREA), creatinine (CRE) and dehydrogenase (LDH), are similar among the control group and the GO-treated groups, except that the significant increase in the UREA, CRE and LDH levels is observed in the multiple-dose l-GO group. The increase of UREA and CRE, which are important indicators of nephritic injury, infers possible kidney injury induced by the multiple-dose-exposure of l-GO. As for the cytoplasmic enzyme LDH, it is an indicator of alveolar macrophage injury in the pulmonary toxicity study, and also a general indicator of hepatic and nephritic injuries. The high level of LDH activity manifests that the organ injury is aroused by the l-GO exposure.

3.4 Histopathological observations

The histological photographs of the lung, liver and kidney tissues are shown in Figs. 2-5. In lungs, many GO aggregates are observed in macrophage nodules after mice were treated with a single-dose of 2.1 mg kg^{-1} s-GO or l-GO, but no other lung damage is observed. No macrophage nodule or other lung damages is observed in mice after the multiple-dose of s-GO treatment. However, small GO enriched macrophage nodules as well as serious inflammation infiltrations are observed in the mice exposed to the multiple-dose of l-GO. The alveolar walls thicken and swell, and the alveolar cavity shrinks (Fig. 2). In addition, the lymphocytes seriously infiltrate smooth muscle layer of bronchioles and vessels in the multiple-dose exposure of l-GO.

However, no thromb is observed, in accordance with the results of the plasma coagulation parameters (Table 2). The apoptosis of the cells in lung sections was tested by the TUNEL method. Similar to the histopathological observations, black and brown lung macrophage nodules are full of GO, as well as lymphocyte infiltrations around the bronchioles are observed in the GO-exposed groups (Fig. 3). However, the apoptosis levels are similar among all the exposure and control groups.

No obvious hepatic damage is found after the single-dose exposure of GO (Fig. 4). But for the multiple-dose exposure of s-GO, there are some small focal-like inflammatory cells that infiltrate around the central venues of the liver. This may be ascribed to the overload of particles in the liver after the low-dose exposure of s-GO.

The histopathological changes of kidneys in the mice are shown in Fig. 5. The serious swelling in the renal glomerulus and the close capsular space are found only in the multiple-dose exposure of l-GO. The remarkable renal tubule injury is in accordance with the plasma biochemical assay (Table 3). No significant change is observed in other groups compared with the control mice. As for spleen, no obvious damage was induced in the GO exposed mice (Fig. S2).

3.5 Oxidative stress

The oxidative stress aroused by the GO samples in main organs was measured to reveal the possible toxicological pathway. However, as shown in Fig. 6, the GSH level and MDA level in liver, spleen and lungs remain unchanged in all groups. Namely, there was no observed oxidative damage to these organs.

3.6 GO in lung tissues

The Raman G-peak signal of GO is at around 1600 cm^{-1}, which is the characteristic of graphite carbon. Under the Raman microscope, paraffin-embedded mouse lung sections show focal increases of G-peak signal in macrophage nodules both in the H-E staining section or the TUNEL section, indicating the enriched GO at the grey ranges (macrophage nodules) (Fig. 7). While, no G-band signal was observed in all control tissue samples (data not shown). This evidences that GO exists in lung macrophage nodules after the GO exposure. The accumulation of GO in lungs was confirmed by spectrometric method (Fig. S3).

4. Discussion

GO exhibits high solubility and stability in physiological solution and has been used in drug delivery, bioimaging etc.[10,30] However, the *in vivo* behavior of graphene-based nanomaterials still remains largely unknown. Herein, the size and dose effects on the toxicity of GO were evaluated in the animal model. The biological consequences of GO exposure in different conditions are summarized in Table 4.

The pulmonary toxicity is a focal point of the toxicity of GO. In fact, GO has shown obvious pulmonary toxicity with different exposure methods.[19,31] GO caused acute and sustained inflammatory response in the lungs and pleural space by the pharyngeal aspiration or direct intrapleural injection.[31] Exposed by the intratracheal injection, lung macrophages with a homogeneous black cytoplasm throughout the lungs were observed, and the GO aggregates induced peribronchial inflammation, alveolar exudates and mild fibrosis in mice.[19] In addition, exposed by the single *i.v.* injection, inflammatory cell

Table 3. Plasma biochemical parameters of the GO-exposed and control mice. Data represent mean±S.D. (n=5).

Animal groups		TBIL (µmol L⁻¹)	ALT (IU L⁻¹)	AST (IU L⁻¹)	ALP (IU L⁻¹)	UA (µmol L⁻¹)	UREA (µmol L⁻¹)	CRE (µmol L⁻¹)	LDH (IU l⁻¹)
Single-dose	Control	6.4 ±0.3	40.2 ±12.1	64.5 ±10.6	75.2 ±11.1	34.4 ±11.7	7.5 ±1.2	15.2 ±3.5	250.6 ± 76.3
	0.3 mg kg⁻¹ s-GO	6.2 ±0.2	32.4 ±9.2	58.7 ±13.4	96.5 ±20.4	26.8 ±9.7	7.8 ±1.5	15.8 ±2.6	229.0± 57.2
	0.3 mg kg⁻¹ l-GO	6.2 ±0.2	33.1 ±3.8	60.9 ±3.0	74.6 ±14.7	29.4 ±9.4	7.4 ±0.6	15.6 ±4.0	284.2± 71.1
	2.1 mg kg⁻¹ s-GO	6.3 ±0.2	31.7 ±5.7	53.0 ±4.6	77.6 ±10.4	38.0 ±14.0	8.7 ±1.0	20.2 ±5.0	237.0± 25.2
	2.1 mg kg⁻¹ l-GO	6.3 ± 0.3	35.4± 7.4	56.5± 5.9	86.8± 13.1	52.2± 38.3	8.1± 1.1	16.8± 4.2	263.0± 72.9
Multiple-dose	Control	6.3±0.3	37.4±12.5	65.0±17.9	73.2±8.6	47.6±28.5	6.6±0.8	15.6±1.1	201.6± 51.2
	0.3 mg kg⁻¹ s-GO	6.3±0.2	31.2±8.7	63.0±5.9	74.5±8.2	42.8±11.2	7.1±2.0	15.5±3.4	237.3± 28.5
	0.3 mg kg⁻¹ l-GO	6.1±0.2	40.8±5.2	65.1±3.8	86.3±11.6	34.3±10.3	9.1±0.7*	18.3±1.7*	274.0± 20.2*

TBIL: total bilruin; ALT: alanine aminotransferase; AST: aspartate aminotrasferase; ALP: alkaline phosphatase; UA: uric acid; CRE: creatinine; LDH: lactate dehydrogenase.

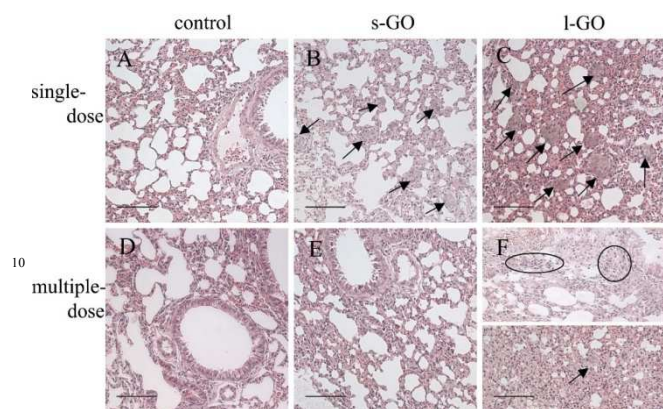Significantly different from the control at P<0.05.

Fig. 2 Representative histopathological changes of the lungs of the GO-exposed and control mice on H&E section. Dose of s-GO and l-GO is 2.1 mg kg⁻¹ for the single-dose exposure and 0.3 mg kg⁻¹ (every other day, totally seven injections) for multiple-dose exposure. The arrows indicate the lung macrophage nodules full of GO; the circles indicate the lymphocyte infiltration around the bronchiole.The scale bar represents 100 µm.
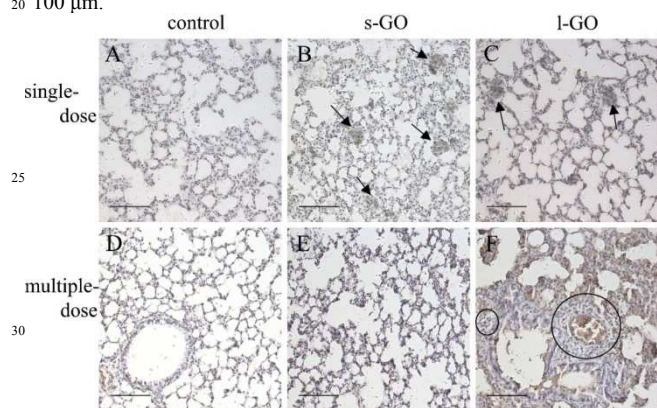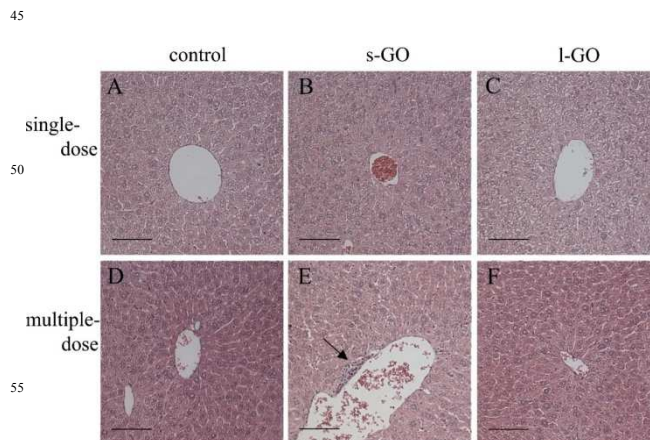

Fig. 4 Representative histopathological changes of the liver of the control and GO exposed mice on H&E section. Dose of s-GO and l-GO is 2.1 mg kg⁻¹ for single-dose exposure and 0.3 mg kg⁻¹ (every other day, totally seven injections) for multiple-dose exposure. Arrow indicates the small focal-like inflammatory cells infiltrate around the central vein. The scale bar represents 100 µm.
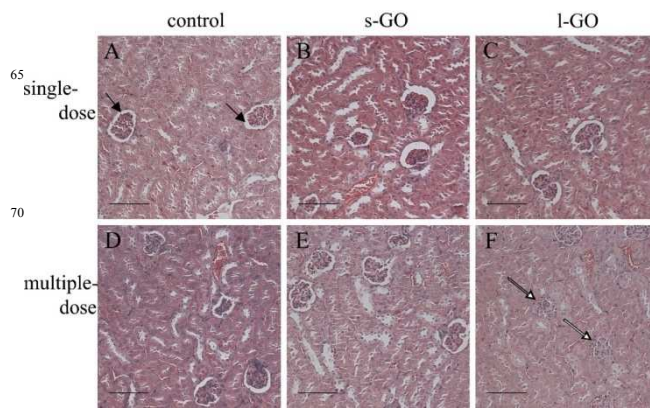

Fig. 3 Apoptosis analysis of the lungs of the GO exposed and control mice by TUNEL method. Dose of s-GO and l-GO is 2.1 mg kg⁻¹ for single-dose exposure and 0.3 mg kg⁻¹ (every other day, totally seven injections) for multiple-dose exposure. The black solid arrows indicate the lung macrophage nodules full of GO; the circles indicate lymphocyte infiltration around the bronchiole. The scale bar represents 100 µm.

Fig. 5 Representative histological changes of the kidneys of the control and GO treated mice on H&E section. Dose of s-GO and l-GO is 2.1 mg kg⁻¹ for single-dose exposure and 0.3 mg kg⁻¹ (every other day, totally seven injections) for multiple-dose exposure. The arrows show the renal glomerulus and renal glomerular capsule interspace. In the multiple-dose l-GO group, the glomerular capsule interspaces disappeared (hollow arrows), which might result from swollen glomerulus cells. The scale bar represents 100 µm.
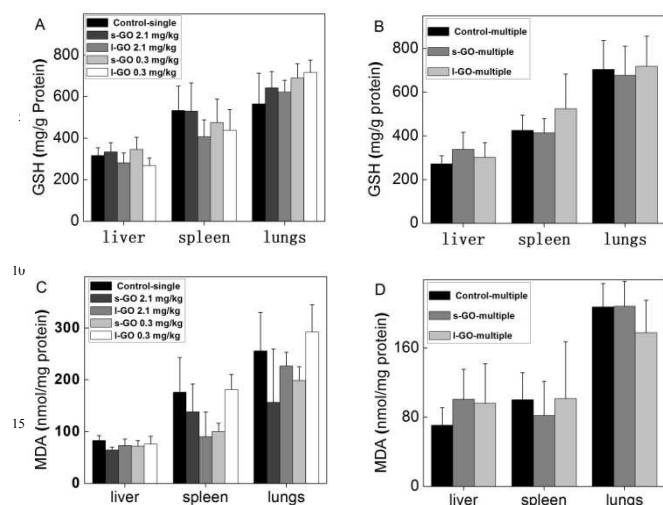
Fig. 6 The oxidative stress of the control mice and the GO exposed mice. (A) GSH level of main organs for multiple-dose groups; (B) GSH level of main organs for single-dose groups; (C) MDA level of main organs for multiple-dose groups. (D) MDA level of main organs for single dose groups.
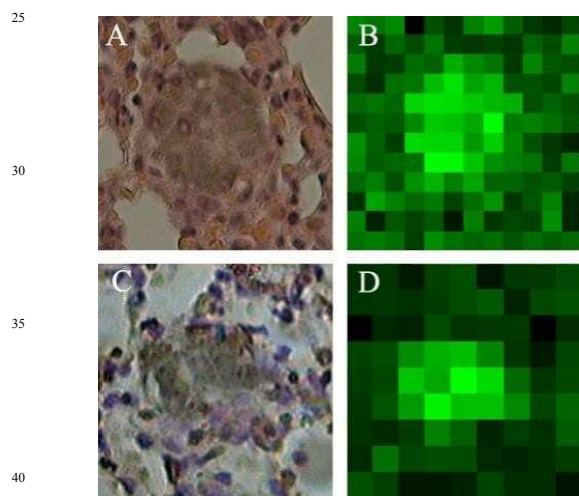

Fig. 7 Micro-Raman mapping of the lung section of the mouse after exposed to single-dose (2.1 mg kg^{-1}) l-GO. The images were obtained in 7 μm × 7 μm steps. (A) The H&E section of lung. (B) The Raman mapping of the same area in (A). (C) The lung section stained by TUNEL method. (D) The Raman mapping of the same area in (C).

infiltration, fibrosis and lung nodule formation in lungs could also be easily observed,[22,32] which is in accordance with our observation. In fact, the formation of macrophage nodules in lungs was generally observed for the animal exposed to the other carbon nanomaterials, such as carbon nanotubes (CNTs). The intratracheal instillation of CNTs induced the formation of granuloma in lungs.[33,34] The similar macrophage nodules could be seen after a single *i.v.* injection of CNTs.[32]

We found that the grey lung macrophage nodules were full of GO by the Raman mapping technique (Fig. 7), which has been widely used to observe single-walled CNTs (SWCNTs) *in vivo*, taking advantage of the evident SWCNTs G-band Raman signal

at ~1580 cm^{-1}.[29] Although the G-band intensity shown in GO is orders of magnitudes lower compared to that of SWCNTs,[35-37] the Raman spectroscopic method has been successfully used to qualitatively track GO in the mouse lungs and liver by measuring their homogenates in our group.[6] Here, for the first time we show the GO distribution in tissue directly, and then associate the accumulation of GO with the pathological changes. The Raman imaging could reveal GO clearly without any interference. For example, the low contrast of GO and the grey color of the stained inflammatory cells under optical microscope may hide the true distribution of GO in tissues. We found that the macrophage nodules were full of GO, but GO did not accumulate in the lymphocyte infiltrated around the bronchioles (data not shown). It

suggested that the lymphocytes recruited by the GO-induced injury were not able to trap GO, though these cells have vigorous phagotrophic ability.

According to our results, the oxidative stress is not the dominant toxicological mechanism of the *i.v.* exposed GO. Although oxidative stress is a broadly existent phenomenon when cells are exposed to GO,[23] the protective effect of existing proteins should be noticed. When GO is incubated with serum, due to the high protein adsorption ability of GO, the interaction between GO sheets and proteins and thus the cytotoxicity of GO are largely attenuated.[38] In such case, the protein adsorption on GO might protect the organs against the oxidative damages.

No significant hepatic index, pathological change and oxidative stress were observed in mice postexposed to GO, except the slightly inflammatory response in the multiple-low-dose exposure of s-GO. It was in consistent with the previous reports that GO could induce slight hepatic toxicity.[12,32] In fact, neither l-GO nor high concentration s-GO distributed considerably in liver.[6]

The low hepatic toxicity of GO was different from our previous report on pristine SWCNTs.[29] SWCNTs increased the levels of serum biochemical parameters indicating the hepatic injury including ALT and AST after the single-dose *i.v.* exposure. But the low hepatic toxicity of GO observed was similar to that of the functionalized SWCNTs with higher hydrophilicity. For example no sign of liver injury was shown in mice at 28 days after the single-dose *i.v.* exposure to taurine functionalized multi-walled CNTs (MWCNTs), even though 78 % of the MWCNTs were found to be accumulated in the liver.[38] In a word, the good hydrophilicity is an important factor for the biocompatibility of GO.

The excretion of l-GO through the kidneys might be one reason for the renal injury. There are also some papers reporting the excretion of GO from the body. Zhang *et al.* found that the clearance of GO from kidneys was size-dependent. Large GO particles were intercepted and then highly accumulated in lungs, while the small size GO quickly eliminated through the renal route.[22] In this study, for the multiple-dose exposure of GO, the renal damage of mice was GO size-dependent, too. The s-GO neither accumulated in the kidneys, nor induced the renal damage.

Paper

Table 4 Biological consequences of GO exposure in different conditions.

Animal groups		Organ indices		Lymphcyte infiltration		Lung microphage nodule		Renal glomerulus swelling	Plasma biochemical parameters
		liver	lungs	liver	lungs	number	size		
Single-dose	0.3 mg kg⁻¹ s-GO								
	0.3 mg kg⁻¹ l-GO								
	2.1 mg kg⁻¹ s-GO					+	++		
	2.1 mg kg⁻¹ l-GO					+	++		
Multiple-dose	0.3 mg kg⁻¹ s-GO	+		+					
	0.3 mg kg⁻¹ l-GO		+		+	++	+	+	+

+ significant toxicity observed.
++ severe toxicity observed.

Similar results were reported by Yang *et al.*, who observed the clearance of the small size PEG functionalized GO (10-30 nm) without obvious kidney damage in mice after the *i.v.* exposure.[36] For l-GO in this paper, the renal damage might be attributed to the failed clearance of the large GO sheets.

"Dose makes poison" is an everlasting truth. Previous studies confirm that the exposure dose is a key factor affects the toxicity of GO, too. Wang *et al.* found that low and middle-dose of GO (0.1 mg and 0.25 mg per mouse, respectively) did not exhibit obvious toxicity in mice, while high-dose of GO (0.4 mg per mouse) induced chronic toxicity, such as lung nodule formation and even death.[32] Zhang *et al.* compared the toxicity of GO in mice at 1.0 mg kg⁻¹ and 10.0 mg kg⁻¹ at 14 days post a single-dose *i.v.* injection, and found that GO was biocompatible in most tissues, including liver, spleen and kidneys, but induced lung pathological changes at the higher dose.[22]

In this work, we also observed the dose effect, by comparing the low and high single-dose exposed groups. At 15 days after the single-low-dose exposure, neither l-GO nor s-GO induced any change in the organ indices or plasma biochemical parameters. But post the single-high-dose exposure of s-GO or l-GO, toxicities, such as the organ indices changes and lung nodule formation were observed.

Given the same total exposure dose (2.1 mg kg⁻¹), the toxicity can also be modulated by changing the exposure frequency. We observed the macrophage nodules induced by GO in the mouse lungs post the single-high-dose exposure of s-GO (2.1 mg kg⁻¹), however, no such nodule was found post the multiple-low-dose exposure of s-GO (0.3 mg kg⁻¹, 7 times), though the total exposure doses were identical. Our previous research has found that the dose could regulate the distribution of GO in mice.[6] Post the single-dose exposure of GO, the accumulation of s-GO in lungs increased with increasing GO dose, because the GO in higher concentration readily interacted with the proteins forming larger GO-protein complexes which might be retained in the lungs. Whereas, the majority of s-GO could pass the lung capillary post each low-dose exposure, the final accumulation of s-GO in lungs post the multiple-low-dose exposure was lower than that of the single-high-dose exposure.

The toxicity of l-GO was modulated by changing the exposure frequency as well. Unlike s-GO, the multiple-low-dose exposure of l-GO made more accumulation of l-GO and hence severer toxicity, even death compared with the single-high-dose exposure of l-GO. One possible mechanism is that l-GO formed larger numbers of smaller GO-protein complexes at lower concentration.[6] These smaller complexes can enter the capillary, create more injury points and hence more inflammatory cells.

The size of GO sheets affected their toxicity. The multiple-dose exposure of l-GO induced serious lymphocyte infiltration around the bronchioles in lungs, as well as obvious renal damage. The multiple-dose exposure of s-GO didn't significantly induce lung or kidney damages, but induced the liver index increase and inflammatory cell infiltration. The size related different distribution behaviours of s-GO and l-GO were clearly demonstrated: s-GO mainly distributed in liver, whereas l-GO in lungs post the low concentration exposure. However, the size effects, on both the biodistribution and toxicity effects of GO, would be hidden by the formation of the large protein-complex at the high concentration.

Conclusions

In this work, the toxicity of s-GO and l-GO post different *i.v.* exposure protocols was examined. The toxicity of GO *i.v.* exposed to mice was tuned by the dose, size and exposure protocols of GO. The single-high-dose exposure (2.1 mg kg⁻¹) of s-GO or l-GO caused the macrophage nodules formation in lungs, and the multiple-low-dose exposure (seven repeated doses of 0.3 mg kg⁻¹) of l-GO also induced small macrophage nodules formation as well as serious lymphocyte infiltration around the bronchioles in lungs and the death of mice. The size is another one key factor influencing the toxicity of GO. The lower toxicity of the multiple-low-dose exposure of s-GO than that of the multiple-low-dose l-GO implicates that GO with smaller size could be more benign to mice. For the biomedical applications in the future, the size and exposure protocols (including dose and dosing frequency) of GO should be optimized and strictly controlled.

Notes and references

a Beijing National Laboratory for Molecular Sciences, College of Chemistry and Molecular Engineering, Peking University, Beijing 100871, China. Tel: 86-10-62757196; E-mail: yliu@pku.edu.cn

b Institute of Nanochemistry and Nanobiology, Shanghai University,

5 *Shanghai 200444, China. Tel: 86-21-66138026; E-mail: hwang@shu.edu.cn*

c Beijing Key Laboratory of Bioprocess, College of Life Science and Technology, Beijing University of Chemical Technology, Beijing, 100029, China

10 *d Department of Clinical Laboratory, Third Hospital of Peking University, Beijing 100083, China*

e Department of Occupational and Environmental Health Sciences, School of Public Health, Peking University, Beijing 100191, China

20 1   L. H. Reddy, J. L. Arias, J. Nicolas, P. Couvreur, *Chem. Rev.*, 2012, **112**, 5818.

2   Committee to Develop a Research Strategy for Environmental, Health, and Safety Aspects of Engineered Nanomaterials, National Research Council, The National Academies Press, Washington, D.C. 25   2012, pp214-219.

3   K. Yang, L. Feng, X. Shi, Z. Liu, *Chem. Soc. Rev.*, 2013, **42**, 530.

4   K. T. Yong, W. C. Law, R. Hu, L. Ye, L. W. Liu, M. T. Swihart, P. N. Prasad, *Chem. Soc. Rev.*, 2013, **42**, 1236.

5   L. M. Kaminskas, B. J. Boyd, C. J. H. Porter, *Nanomedicine*, 2011, **6**, 30   1063.

6   J.-H. Liu, S.-T. Yang, H. Wang, Y. Chang, A. Cao, Y. Liu, *Nanomedicine*, 2012, **7**, 1801.

7   Armida, M. M. Janat-Amsbury, A. Ray, C. M. Peterson, H. Ghandehari, *Eur. J. Pharm. Biopharm.*, 2011, **77**, 417.

35 8   D. Chen, H. Feng, J. Li, *Chem. Rev.*, 2012, **112**, 6027.

9   K. S. Novoselov, A. K. Geim, S. V. Morozov, D. Jiang, Y. Zhang, S. V. Dubonos, I. V. Grigorieva, A. A. Firsov, *Science*, 2004, **306**, 666.

10   L. M. Zhang, J. G. Xia, Q. H. Zhao, L. W. Liu, Z. J. Zhang, *Small*, 2010, **6**, 537.

40 11   W. Zhang, Z. Y. Guo, D. Q. Huang, Z. M. LIu, X. Guo, H. Q. Zhong, *Biomaterials*, 2011, **32**, 8555.

12   Y. Wang, Z. Liu, J. Wang, J. Liu, Y. Lin, *Trends Biotechnol.*, 2011, **29**, 205.

13   Y. Z. Pan, N. G. Sahoo, L. Li, *Expert Opin. Drug Delivery*, 2012, **9**, 45   1365.

14   H. Hong, K. Yang, Y. Zhang, J. W. Engle, L. Feng, Y. Yang, T. R. Nayak, S. Goel, J. Bean, C.P. Theur, T. E. Barhart, Z. Liu, W. Cai, *ACS Nano*, 2012, **6**, 2361.

15   K.-H. Liao, Y.-S. Lin, C. W. Macosko, C. L. Haynes, *ACS Appl.* 50   *Mater. Interface*, 2011, **3**, 2607.

16   W. Paul, C. P. Sharma, *Trends Biomater. Artif. Organs*, 2011, **25**, 91.

17   A. A. Sasidharan, L. S. Panchakarla, A. R. Sadanandan, A. Ashokan, P. Chandran, C. M. Girish, D. Menon, S. V. Nair, C. N. R. Rao, M. Koyakutty, *Small*, 2012, **8**, 1251.

55 18   K. Yang, J. M. Wan, S. Zhang, B. Tian, Y. J. Zhang, *Biomaterials*, 2012, **33**, 2206.

19   M. C. Duch, G. R. S. Budinger, Y. T. Liang, S. Soberanes, D. Urich, S. E. Chiarella, L. A. Campochiaro, A. Gonzalez, N. S. Chandel, M. C. Hersam, G. M. Mutlu, *Nano Lett.*, 2011, **11**, 5201.

60 20   S. K. Singh, M. K. Singh, M. K. Nayak, S. Kumari, S. Shrivastava, J. J. A. Gracio, D. Dash, *ACS Nano*, 2011, **5**, 4987.

21   S. K. Singh, M. K. Singh, P. P. Kulkarni, V. K. Sonkar, J. J. A. Gracio, D. Dash, *ACS Nano*, 2012, **6**, 2731.

22   X. Y. Zhang, J. L. Yin, C. Peng, W. Q. Hu, Z. Y. Zhu, W. X. Li, C. 65   H. Fan, Q. Huang, *Carbon*, 2011, **49**, 986.

23   Y. L. Chang, S.-T. Yang, J.-H. Liu, E. Dong, Y. W. Wang, A. Cao, Y. Liu, *Toxicol. Lett.*, 2011, **200**, 201.

24   Y. He, Y. Lin, H. W. Tang, D. W. Pang. *Nanoscale*, 2010, **4**, 2054.

25   C. Lasagna-Reeves, D. Gonzalez-Romero, M. A. Barria, I. Olmedo, 70   A. Clos, V. M. S. Ramanujam, A. Urayama, L. Vergara, M. J. Kogan, C. Soto. *Biochem. Biophys. Res. Commun.*, 2010, **393**, 649.

26   K. Inoue, R. Yanagisawa, E. Koike, M. Nishikawa, H. Takano. *Free Radical Biol. Med.*, 2010, **48**, 924.

27   A. M. Pinto, I. C. Goncalves, F. D. Magalhaes. *Colloids Surf., B*, 75   2013, **111**, 188.

28   A. M. Jastrzebska, P. Kurtycz, A. R. Olszyna. *J. Nanopart. Res.*, 2013, **14**, 1320.

29   S.-T. Yang, X. Wang, G. Jia, Y. Gu, T. Wang, H. Nie, C. Ge, H. Wang, Y. Liu, *Toxicol. Lett.*, 2008, **181**, 182.

80 30   L. Zhou, W. Wang, J. Tang, J. H. Zhou, H. J. Jiang, J. Shen, *Chem. Eur. J.*, 2011, **17**, 12084.

31   A. Schinwald, F. A. Murphy, A. Jones, W. MacNee, K. Donaldson, *ACS Nano*, 2011, **6**, 736.

32   K. Wang, J. Ruan, H. Song, J. Zhang, Y. Wo, S. Guo, D Cui, 85   *Nanoscale Res. Lett.*, 2011, **6**, 1.

33   D. B. Warheit, B. R. Laurence, K. L. Reed, D. H. Roach, G. A. M. Reynolds, T. R. Webb, *Toxicol. Sci.*, 2004, **77**, 117.

34   C. W. Lam, J. T. James, R. McCluskey, R. L. Hunter, *Toxicol. Sci.*, 2004, **88**, 126.

90 35   Z. Liu, C. DAvis, W. Cai, L. He, X. Chen, H. Dai, *Proc. Natl. Acad. Sci.*, 2008, **105**, 1410.

36   K. Yang, J. Wan, S. Zhang, Y. Zhang, S.-T. Lee, Z. Liu, *ACS Nano*, 2010, **5**, 516.

37   K. N. Kudin, B. Ozbas, H. C. Schniepp, R. K. Prud'homme, I. A. 95   Aksay, R. Car, *Nano Lett.*, 2007, **8**, 36.

38   W. Hu, C. Peng, M. Lv, X. Li, Y. Zhang, N. Chen, C. Fan, Q. Huang. *ACS Nano*, 2011, **5**, 3693.

39   X. Y. Deng, S.-T. Yang, H. Y. Nie, H. Wang, Y. Liu, *Nanotechnology*, 2008, **19**, 075101.

100